MULTIPATH RADAR TRACKING WITH LARGE UNCERTAINTY IN THE ENVIRONMENT

Sachintha Karunaratne[⋆] *Mark R. Morelande*[†] *Bill Moran*[†]

[⋆] Department of Electrical and Electronic Engineering, The University of Melbourne, Australia
[†] School of Electrical and Computer Engineering, RMIT University, Australia
Email: {sachi84,m.morelande}@gmail.com,bill.moran@rmit.edu.au

ABSTRACT

We formulate the target tracking problem for radar in a multipath environment where significant uncertainty on the locations of the multipath causing obstacles (walls) is present. Most of the recent efforts towards investigating target tracking in multipath environments assume knowledge of these wall locations. Relaxing this assumption makes the tracking problem very challenging. We propose a statistical filter (tracker) and a data association method based on importance sampling to address these challenges.

Index Terms— Multipath Radar, Importance sampling, Bayesian

1 Introduction

Target tracking in a multipath environment has recently been a highly researched topic among the statistical signal processing research community. This is mainly motivated by its applications in areas such as defence, autonomous navigation, and communication.

Many interesting approaches have been used by researchers in investigating the problem of estimation/detection in a multipath environment where the geometry of the surveillance area is known [1, 2, 3, 4, 5, 6, 7]. As a summary, most of this work consider an environment where the number of obstacles is limited or configured in a special way, e.g., parallel walls. The work done by us using raw sensor measurements to track a target in an urban terrain where walls are not necessarily parallel to each other can be found in [8, 9, 10]. A natural extension of our previous work was to investigate the problem of tracking in a multipath environment where a large uncertainty about the environment prevails. This paper describes the work done towards that end.

Our task of tracking in an uncertain multipath environment closely resembles the well established Simultaneous Localisation and Mapping (SLAM) problem appearing in the domain of robotics and control research [11, 12]. However, the difference between the SLAM and tracking in an uncertain multipath environment comes from the measurement model used; much of SLAM uses LiDAR technology where multipath is not relevant. For the problem considered in this paper, the relationship between the measurements and the environment is more indirect than in conventional SLAM setups.

Some recent work on radar tracking in an unknown multipath environment is found in [13]. The problem considered there is to track a moving radio frequency emitter. The data associations are performed using the well known Viterbi algorithm. The associations are achieved via a maximum likelihood method. The authors take a suboptimal approach of using only the predicted target state when evaluating the cost function for the Viterbi algorithm. The disadvantage of this approximation is that, if the process covariance is broad, the chances of the true target state being significantly different from the predicted are high, and hence inaccurate association weights.

In this paper, we present our work on tracking a target in a highly uncertain multipath environment where the radar system (both the transmitter and the receiver) is not collocated with the target. It is assumed that, a priori, not much information about the location of the walls is available; hence the large uncertainty about the environment. The tracking problem proved to be vary challenging, due to: large uncertainty in the environment and the data association problem.

The brute force calculation of all the association probabilities is computationally very expensive and thus we use an importance sampling procedure to draw samples from association events. The posterior moments conditioned on the sampled association events are also calculated using a Monte Carlo approach. Finally, the state estimate is obtained by averaging the conditional posteriors over association probabilities. Special care is needed in fusing the mixture of conditional posterior distributions. This is due to the implicit ordering in a vector representation, which results in unnecessary confusion between the labels assigned to the walls. Conventional data association algorithms such as Probabilistic Data Association Filter (PDAF) [14] or Joint Probabilistic Data Association Filter (JPDAF) [14] do not address this problem. We used the Set JPDAF (SJPDAF) method suggested in [15] to address the issue which yields more accurate Gaussian approximations. Because it is desired to focus on the problems posed by an unknown environment, we analyse the case where the environment contained two walls and assume in this work perfect detections with no false alarms.

The rest of the paper is organised as follows. We introduce the process and measurement models in Section 2. The estimation problem is also formulated in that section. The methodology is then presented in Section 3. Simulation examples along with a discussion are presented in Section 4 followed by concluding remarks.

2 Modelling and notation

Consider a surveillance area pixelated as a $K \times K$ grid. Two walls are located within this surveillance area. The (linear) walls are represented by slope-intercept pairs $[\alpha_i, \beta_i]$ ($i = 1, 2$) corresponding to the line:

$$x \cos \alpha - y \sin \alpha + \beta = 0.$$

A point target is moving across the surveillance region and the kinematic state of it at discrete time k is denoted by $\mathbf{T}_k$. $\mathbf{T}_k$ consists of position and velocity information in the Cartesian plane; that is,

$$\mathbf{T}_k = [x_k \; \dot{x}_k \; y_k \; \dot{y}_k]',$$

This work was supported by the US Air Force Office of Scientific Research (AFOSR) grant via Arizona State University FA9550-12-1-0418.

where $(x_k, y_k) \in \mathcal{R}^2$ is the position of the target and the dot notation denotes differentiation with respect to time. Without loss of generality, we consider the origin $(0,0)$ to be the bottom left most point of the surveillance region. A radar transmitter and a receiver are located at known positions within the surveillance region to collect measurements for use in localizing the target. Note that one of the limitations of our representation is that we assume the wall to exist throughout the intersection between the straight line represented by the wall parameters and the surveillance area. We believe that the extension to the general case involving line segments could be developed based on the foundations laid out in this paper.

2.1 State dynamics

The kinematic state of the target is assumed to transition from time $k-1$ to k according to the following stochastic model:

$$\mathbf{T}_k = \mathbf{F}\mathbf{T}_{k-1} + \mathbf{v}_k, \tag{1}$$

where

$$\mathbf{F} = \mathbf{I}_2 \otimes \begin{bmatrix} 1 & 1 \\ 0 & 1 \end{bmatrix} \text{ and } \mathbf{v}_k \sim \mathcal{N}(\cdot; \mathbf{0}, \mathbf{Q}), \tag{2}$$

with the symbols $\otimes$, $\mathbf{I}$, and $\mathbf{0}$ denoting the Kronecker operator, Identity matrix, and Zero matrix of appropriate dimensions respectively, and $\mathcal{N}(\cdot; , \boldsymbol{\mu}, \boldsymbol{\Sigma})$ the usual notation for the Gaussian distribution.

The wall parameters are modelled as static random parameters. Additionally the wall parameters for the two walls are independent of each other. If it is assumed that all the possible lines passing through the surveillance area are equally likely to be a wall, then it can be shown that the first two moments of a prior distribution satisfying this requirement are given by:

$$\text{Mean } (\alpha, \beta) = \begin{bmatrix} \frac{\pi}{2} \\ -\frac{k}{\pi} \end{bmatrix} \text{ and Cov } (\alpha, \beta) = \begin{bmatrix} \dfrac{\pi^2}{12} & -\dfrac{k}{\pi} \\ -\dfrac{k}{\pi} & \dfrac{k^2(2\pi^2 - 6 + \pi)}{6\pi^2} \end{bmatrix} \tag{3}$$

We use a normal distribution with the above moments as a prior distribution for the wall parameters. The state vector $\mathbf{x}_k$ at time k consists of both the target dynamics and wall parameters; that is,

$$\mathbf{x}_k = [\mathbf{T}'_k \ \alpha_1 \ \beta_1 \ \alpha_2 \ \beta_2]'. \tag{4}$$

2.2 Measurements

The measurements at time k consist of range (r) and Angle of Arrival (AOA) (θ) of each multipath and the direct path. We define a multipath as a path from the transmitter to the radar sensor which has been in contact with the target as well as at least with one wall. Any path that has hit a wall more than twice is ignored in the model under the assumption that such paths are subject to severe attenuation in signal power. We assume that the walls act as specular reflectors and that necessary processing has been carried out to reject clutter measurements.

The measurement vector at time k for N paths is given by:

$$\mathbf{y}_k = [\mathbf{r}'_{1,k} \ \mathbf{r}'_{2,k} \dots \ \mathbf{r}'_{N,k}]' + \mathbf{u}_k = [\mathbf{y}'_{1,k} \ \mathbf{y}'_{2,k} \dots \ \mathbf{y}'_{N,k}]', \tag{5}$$

where

$\mathbf{r}_{i,k} = [r_{i,k} \ \theta_{i,k}]'$ denotes a vector containing (noiseless) range and AOA of the i^{th} path at time k,

$\mathbf{u}_k \sim \mathcal{N}(\cdot; \mathbf{0}; \mathbf{R})$ is the measurement noise,

$\mathbf{y}_{i,k}$ is the vector containing the range and AOA of the i^{th} multipath at time k.

The noise covariance matrix $\mathbf{R}$ is:

$$\mathbf{R} = \mathbf{I}_N \otimes \begin{bmatrix} \sigma_r^2 & 0 \\ 0 & \sigma_\theta^2 \end{bmatrix}.$$

We assume that all the possible paths arising from reflections from the two walls exist at time k.

2.3 Path configurations and the measurement association vector

A path can be decomposed into two segments: the forward path from the transmitter to the target and the reverse path from the target to the sensor. Assume that at most one wall is hit in each segment. Thus a path is uniquely identified by two numbers given by the labels of the walls that were hit in each segment respectively. If a wall is not hit on a particular segment, then that segment would be identified by '0'. We denote this pair of non-negative integers identifying a path as a *path configuration*.

Note that for a 2 wall environment, 9 distinct path configurations exist. Let the 9×2 matrix $\mathbf{C}$ denote the collection of all the path configurations, where the i^{th} row $\mathbf{C}_i$ contains the ordered pair of numbers identifying the i^{th} path configuration; that is,

$$\mathbf{C} = \begin{bmatrix} 0 & 1 & 2 & 0 & 0 & 1 & 1 & 2 & 2 \\ 0 & 1 & 2 & 1 & 2 & 2 & 0 & 0 & 1 \end{bmatrix}'. \tag{6}$$

By itself the measurement vector $\mathbf{y}_k$ does not provide information about how the measurements are associated with path configurations. The association vector $\mathbf{e}_k$ provides the mapping between measurements and path configurations. Let $\mathbf{e}_k \in \mathcal{S}_9$ (set of permutations of integers $1, 2, \dots, 9$). Then, the i^{th} element of $\mathbf{e}_k$, denoted by $e_{i,k}$ maps the path configuration represented by the i^{th} row of $\mathbf{C}$ to the $e_{i,k}^{th}$ measurement $\mathbf{y}_{e_{i,k},k}$ at time k.

2.4 Estimation problem

Let $\mathbf{y}^k = [\mathbf{y}'_1 \ \mathbf{y}'_2 \ \dots \ \mathbf{y}'_k]'$ denote the vector of measurements up to time k. We are interested in estimating the state vector $\mathbf{x}_k$ upon observing $\mathbf{y}^k$ and in particular the posterior density $p(\mathbf{x}_k|\mathbf{y}^k)$.

3 Method

It is convenient to define the following indexing notations which will be used to describe the methodolody.

$$1 : j := [1 \ 2 \ \dots \ j]' \text{ where } j \in \mathbb{Z}^+ \tag{7}$$

$$\mathbf{x}_\mathbf{v} := [x_{v_1} \ x_{v_2} \dots \ x_{v_N}] \text{ where } x_n \text{ is the } n^{th} \text{element of } \mathbf{x} \text{ and the index vector } \mathbf{v} \text{ consist of } N \text{ integer indices.} \tag{8}$$

Consider the posterior distribution of the target state $\mathbf{x}_k$:

$$p(\mathbf{x}_k|\mathbf{y}^k) = \sum_{\mathbf{e}_k} p(\mathbf{x}_k|\mathbf{y}^k, \mathbf{e}_k) p(\mathbf{e}_k|\mathbf{y}^k). \tag{9}$$

First, we concentrate on the posterior probability for an association hypothesis $p(\mathbf{e}_k|\mathbf{y}^k)$:

$$p(\mathbf{e}_k|\mathbf{y}^k) \propto p(\mathbf{y}_k|\mathbf{e}_k, \mathbf{y}^{k-1}) p(\mathbf{e}_k|\mathbf{y}^{k-1}), \tag{10}$$

$$= \prod_{n=1}^{N} p_n(\mathbf{y}_{e_n,k}|\mathbf{y}^{k-1}), \tag{11}$$

where $N = 9$ is the number of path configurations, and

$$p_n(\mathbf{y}_{e_{n,k},k}|\mathbf{y}^{k-1}) := p(\mathbf{y}_{e_{n,k},k}|\mathbf{e}_{1:n,k}, \mathbf{y}_{\mathbf{e}_{1:n-1,k},k}, \mathbf{y}^{k-1}). \tag{12}$$

Note that we have assumed $p(\mathbf{e}_k|\mathbf{y}^{k-1}) = p(\mathbf{e}_k)$ is a uniform prior distribution in deriving (11).

An optimal implementation of the filter using (9) and the posterior association probability (11) is not possible because there are too many association hypotheses $\mathbf{e}_k$, as well as intractable integrals. Procedures for addressing these issues are discussed next.

Assume that we have at our disposal, a sample approximation $\hat{p}(\mathbf{x}_k|\mathbf{e}_{1:n-1}, \mathbf{y}_{\mathbf{e}_{1:n-1},k}, \mathbf{y}^{k-1})$, which approximates the distribution $p(\mathbf{x}_k|\mathbf{e}_{1:n-1}, \mathbf{y}_{\mathbf{e}_{1:n-1},k}, \mathbf{y}^{k-1})$. Then, using Chapman-Kolmagarov formula and Monte Carlo sampling, we approximate:

$$p_n(\mathbf{y}_{e_n,k}|\mathbf{y}^{k-1}) \approx \frac{1}{M} \sum_{m=1}^{M} p_n(\mathbf{y}_{e_n,k}|\mathbf{x}_k^{(n,m)}, \mathbf{y}^{k-1}), \tag{13}$$

where $\mathbf{x}_k^{(n,m)} \sim \hat{p}(\mathbf{x}_k|\mathbf{e}_{1:n-1}, \mathbf{y}_{\mathbf{e}_{1:n-1},k}, \mathbf{y}^{k-1})$.

The approximate distribution $\hat{p}(\mathbf{x}_k|\mathbf{e}_{1:n-1}, \mathbf{y}_{\mathbf{e}_{1:n-1},k}, \mathbf{y}^{k-1})$ that was used to draw samples in (13) can be updated to $\hat{p}(\mathbf{x}_k|\mathbf{e}_{1:n}, \mathbf{y}_{\mathbf{e}_{1:n},k}, \mathbf{y}^{k-1})$ as shown by (14), which satisfies the recursive dependence required to evaluate $p_{n+1}(\cdot)$:

$$\hat{p}(\mathbf{x}_k|\mathbf{e}_{1:n}, \mathbf{y}_{\mathbf{e}_{1:n},k}, \mathbf{y}^{k-1}) \propto \sum_{m=1}^{M} p_n(\mathbf{y}_{e_n,k}|\mathbf{x}_k^{(n,m)}, \mathbf{y}^{k-1}) \delta(\mathbf{x}_k - \mathbf{x}_k^{(n,m)}). \tag{14}$$

In the implementation, we improved the sample approximation (14) by introducing resampling and regularisation [16] and the resulting distribution is summarised as a Gaussian (by matching the sample mean and covariance). Additionally, we used the method of progressive correction as in [17], which proved to be invaluable in the presence of large uncertainty in the environment. Space restrictions inhibit us from being more descriptive on these improvements.

Again, consider $p(\mathbf{e}_k|\mathbf{y}^k)$. We use (13) in (11) to approximate the posterior distribution for the association vector as:

$$p(\mathbf{e}_k|\mathbf{y}^k) \propto \prod_{n=1}^{N} \sum_{m=1}^{M} p_n(\mathbf{y}_{e_n,k}|\mathbf{x}_k^{(n,m)}, \mathbf{y}^{k-1}). \tag{15}$$

Drawing a sample directly from (15) is not computationally feasible because of the enormous number of possible hypotheses. Hence we now present an importance distribution $q(\mathbf{e}_k|\mathbf{y}_k)$ to draw association vector samples.

First, define $f_n(\mathbf{x}_k, \mathbf{y}^k, \mathbf{e}_{1:n-1}, v)$:

$$f_n(\mathbf{x}_k, \mathbf{y}^k, \mathbf{e}_{1:n-1}, v) := p_n(\mathbf{y}_{v,k}|\mathbf{e}_{1:n-1}, e_n = v, \mathbf{x}_k^{(n,m)}, \mathbf{y}^{k-1}) \quad \text{where } v \in \mathcal{A}_n, \tag{16}$$

with $\mathcal{A}_n := \{1, 2, \ldots, N\} \backslash \{e_1, e_2, \ldots, e_{n-1}\}$. Now, define the importance density $q(\mathbf{e}_k|\mathbf{y}^k)$ as:

$$q(\mathbf{e}_k|\mathbf{y}^k) = \prod_{n=1}^{N} \left(\frac{\sum_{m=1}^{M} f_n(\mathbf{x}_k^{(n,m)}, \mathbf{y}^k, \mathbf{e}_{1:n-1}, v) \text{ where } v \in \mathcal{A}_n}{\sum_{v \in \mathcal{A}_n} \sum_{m=1}^{M} f_n(\mathbf{x}_k^{(n,m)}, \mathbf{y}^k, \mathbf{e}_{1:n-1}, v)} \right), \tag{17}$$

In the context of importance sampling, the samples obtained from $q(\mathbf{e}_k|\mathbf{y}^k)$ are assigned a weight $\tilde{\phi}$ given by:

$$\tilde{\phi} = p(\mathbf{e}_k|\mathbf{y}^k)/q(\mathbf{e}_k|\mathbf{y}^k), \tag{18}$$

$$\propto \prod_{n=1}^{N} \sum_{v \in \mathcal{A}_n} \sum_{m=1}^{M} p_n(\mathbf{y}_{v,k}|\mathbf{e}_{1:n-1}, e_n = v, \mathbf{x}_k^{(n,m)}, \mathbf{y}^{k-1}). \tag{19}$$

We obtain the posterior densirty for the target state:

$$p(\mathbf{x}_k|\mathbf{y}^k) = \int p(\mathbf{x}_k|\mathbf{y}^k, \mathbf{e}_k) p(\mathbf{e}_k|\mathbf{y}^k) d\mathbf{e}_k, \tag{20}$$

$$\overset{\sim}{\propto} \sum_{j=1}^{J} \tilde{\phi}_j \hat{p}(\mathbf{x}_k|\mathbf{e}_k^{(j)}, \mathbf{y}^k), \tag{21}$$

where

$$\mathbf{e}_k^{(j)} \sim q(\mathbf{e}_k|\mathbf{y}^k), \tag{22}$$

$$\tilde{\phi}_j \propto \prod_{n=1}^{N} \sum_{v \in \mathcal{A}_{n,j}} \sum_{m=1}^{M} p_n(\mathbf{y}_{v,k}|\mathbf{e}_{1:n-1}^{(j)}, e_n = v, \mathbf{x}_k^{(n,m)}, \mathbf{y}^{k-1}), \tag{23}$$

with $\mathcal{A}_{n,j}$ given by:

$$\mathcal{A}_{n,j} = \{1, 2, \ldots, N\} \backslash \{e_1^{(j)}, e_2^{(j)}, \ldots, e_{n-1}^{(j)}\}. \tag{24}$$

3.1 The need for the Set JPDAF

A common problem with data association algorithms such as PDAF, JPDAF, and Multiple Hypothesis Tracking (MHT) filter [18] is the requirement of these algorithms to retain the label assigned to each target throughout the trajectory. This is a consequence of the implicit labelling when parameter vectors are concatenated into a vector. As an illustration of the problem observe that the association vector samples $\mathbf{e}_k^{(1)}$ and $\mathbf{e}_k^{(2)}$ given below represent the same physical mapping, if the labels of the walls are swapped under any one of those hypothesis:

$$\mathbf{e}_k^{(1)} = [2\ 9\ 4\ 3\ 5\ 1\ 6\ 8\ 7]', \qquad \mathbf{e}_k^{(2)} = [2\ 4\ 9\ 5\ 3\ 7\ 8\ 6\ 1]'. \tag{25}$$

The consequences of this effect on the estimates are significant. Consider the posterior estimates of just the slope parameters of the two walls (that is, α_1 and α_2). Assume that the true slope parameters are given by $\pi/4$ and $-\pi/6$. For the purpose of demonstration we restrict the number of $\mathbf{e}_k$ samples to just the 2 samples $\mathbf{e}_k^{(1)}$ and $\mathbf{e}_k^{(2)}$ explicitly given in (25). Further, assume that the two hypotheses are equally weighted; that is, $\tilde{\phi}_1 = \tilde{\phi}_2 \propto .5$. Finally assume that the conditional posteriors are given by the following two equations:

$$\hat{p}(\alpha_1, \alpha_2|\mathbf{e}_k^{(1)}, \mathbf{y}^k) = \mathcal{N}\left(\cdot; \begin{bmatrix} 0.74 \\ -0.49 \end{bmatrix}, 0.01\mathbf{I}_2\right) \tag{26}$$

$$\hat{p}(\alpha_1, \alpha_2|\mathbf{e}_k^{(2)}, \mathbf{y}^k) = \mathcal{N}\left(\cdot; \begin{bmatrix} -0.55 \\ 0.8 \end{bmatrix}, 0.01\mathbf{I}_2\right) \tag{27}$$

The contour plot for the posterior obtained by substituting (26) and (27) into (21) is shown in Figure 1(a). It is evident that the posterior is bimodal. Therefore, the posterior mean, given by $[0.095\ 0.155]'$, is quite distant from the true value and a Gaussian, as used in JPDAF, is a poor approximation to the posterior.

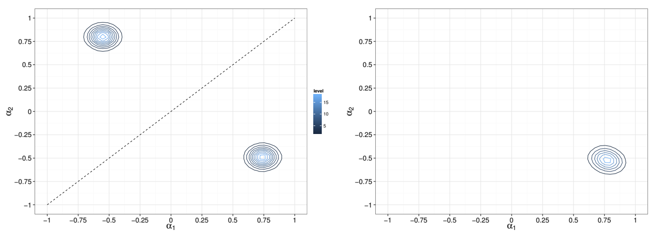

(a) (b)

Fig. 1: Contour plot of $p(\alpha_1, \alpha_2|\mathbf{y}_k)$: (a) before label switching (b) after label switching.

Suppose now, we exchange the wall labels under the data association hypothesis $\mathbf{e}_k^{(2)}$. Then the conditional posteriors are:

$$\hat{p}(\alpha_1, \alpha_2|\mathbf{e}_k^{(1)}, \mathbf{y}^k) = \mathcal{N}\left(\cdot; \begin{bmatrix} 0.74 \\ -0.49 \end{bmatrix}, 0.01\mathbf{I}_2\right) \tag{28}$$

$$\hat{p}(\alpha_1, \alpha_2|\mathbf{e}_k^{(2)}, \mathbf{y}^k) = \mathcal{N}\left(\cdot; \begin{bmatrix} 0.8 \\ -0.55 \end{bmatrix}, 0.01\mathbf{I}_2\right) \tag{29}$$

The contour plot for the posterior distribution after label switching is given in Figure 1(b). Note that the posterior approximation after label switching is much closer to the true parameters. Of course we could have alternatively exchanged the labels under $\mathbf{e}_k^{(1)}$ instead of $\mathbf{e}_k^{(2)}$ and obtained $[-0.52\ 0.77]'$ as the posterior mean, which is equally acceptable because we are only interested in knowing where the walls are. A modification to the traditional JPDAF algorithm with the emphasis on label switching to solve the above problem is known as Set-JPDAF [15]. We have incorporated SJPDAF in the context of the mixture appearing in (21).

4 Results and discussion

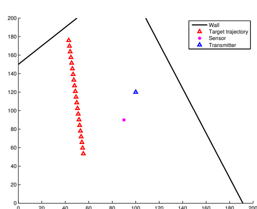

Fig. 2: Multipath environment.

Consider the simulation setup depicted in Figure 2, where K is set to 200. The two walls are represented by the parameters (α, β) given by $[\pi/4\ 150\cos(\pi/4)]'$ and $[5\pi/8\ 250\cos(3\pi/4)]'$ respectively. The coordinates of the radar transmitter and receiver are $(100, 120)$ and $(90, 90)$ respectively. The initial prior for the target kinematic state $\mathbf{T}_0$ is a multivariate normal with mean $[60\ 0\ 50\ 5]'$ and the covariance matrix is diagonal with the diagonal elements given by $[9\ 1\ 9\ 1]'$. The covariance matrix $\mathbf{Q}$ for the process noise is:

$$\mathbf{Q} = \begin{bmatrix} \kappa_1 & 0 \\ 0 & \kappa_2 \end{bmatrix} \otimes \begin{bmatrix} \frac{(\Delta T)^3}{3} & \frac{(\Delta T)^2}{2} \\ \frac{(\Delta T)^2}{2} & \Delta T \end{bmatrix}, \tag{30}$$

where $\kappa_1 = \kappa_2 = 0.5$ and the state sampling interval $\Delta T = 1$. Measurement noise parameters are set by $\sigma^2 = 1$ and $\sigma_\theta = \pi/90$.

We tested the filter against two separate prior distributions for the wall parameters. The first is a normal approximation using the moments (3). Let this prior be denoted by $p_{w,1}(\cdot)$. The second prior $p_{w,2}(\cdot)$ is less uncertain about the environment compared to $p_{w,1}(\cdot)$. To put the level of uncertainty assumed by the prior distributions in some context, note that for $p_{w,1}$, the standard deviation (of the marginal distributions) for the intercept (β) is approximately 106.8 and for the angle parameter (α) is approximately 52 degrees. The corresponding numbers for $p_{w,2}$ are 70 and 30 respectively.

The number J of association samples drawn is fixed at 300 for the simulations appearing in this section. Further, all the simulation results that follow are produced by Monte Carlo using 150 realisations of each experiment. The filter was run against various uncertainty levels ranging from a deterministic environment (wall parameters are known) through to $p_{w,2}$ and $p_{w,1}$. The results are shown in Figure 3(a). By observing the three curves in Figure 3(a) which had

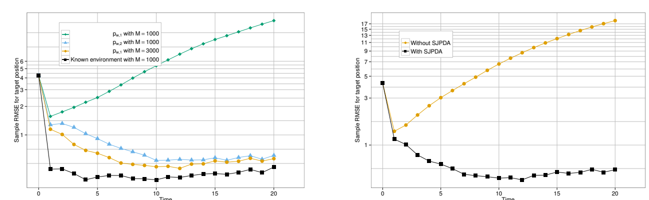

(a) (b)

Fig. 3: (a) Assessing the effect of uncertainty on the filter performance. (b) Assessing the effectiveness of SJPDAF.

used $M = 1000$ samples, we conclude that the results confirm the intuition that larger uncertainty makes the tracking problem harder. In fact with $M = 1000$ for $p_{w,1}$ the filter loses the track. However increasing the sample size to $M = 3000$ produces good results even for the prior with the largest uncertainty $p_{w,1}$. The prior $p_{w,1}$ with $M = 3000$ was used to assess the contribution of the SJPDAF algorithm and the result is illustrated in Figure 3(b). The algorithm failed when the SJPDAF was not used, which is not surprising due to the reasoning in Section 3.1.

5 Conclusion

We have addressed a challenging problem of tracking a target in a highly uncertain multipath environment. An importance sampling based filter is proposed to solve the tracking problem. In particular, the proposed method is able to avoid the typical exhaustive calculation involving a summation over the potentially large number of possible data association hypotheses. We incorporated the Set Joint Probabilistic Data Association filter to address a common labelling problem linked to conventional data association algorithms. Though we have assumed a clutter free model with two walls, the framework presented can be extended to incorporate clutter and multiple unknown walls.

6 References

[1] B. Chakraborty, Y. Li, J.J. Zhang, T. Trueblood, A. Papandreou-Suppappola, and D. Morrell, "Multipath exploitation with adaptive waveform design for tracking in urban terrain," in *IEEE International Conference on Acoustics, Speech and Signal Processing (ICASSP)*, 2010, pp. 3894–3897.

[2] B. Chakraborty, J.J. Zhang, A. Papandreou-Suppappola, and D. Morrell, "Urban terrain tracking in high clutter with waveform-agility," in *IEEE International Conference on Acoustics, Speech and Signal Processing (ICASSP)*, 2011, pp. 3640–3643.

[3] J.L. Krolik, J. Farrell, and A. Steinhardt, "Exploiting multipath propagation for GMTI in urban environments," in *IEEE Conference on Radar*, 2006, p. 4 pp.

[4] H T Hayvaci, Antonio De Maio, and D Erricolo, "Performance analysis of diverse GLRT detectors in the presence of multipath," in *IEEE Radar Conference (RADAR)*, 2012, pp. 902–906.

[5] H T Hayvaci, P Setlur, and N Devroye, "Maximum likelihood time delay estimation and Cramer-Rao bounds for multipath exploitation," *IEEE Radar Conference (RADAR)*, pp. 764–768, 2012.

[6] P. R Barbosa, "Multitarget-multisensor tracking in an urban environment: A closed-loop approach," *Signal and Data Processing of Small Targets*, vol. 6969, pp. W9690–W9690, 2008.

[7] G W Pulford and R J Evans, "A multipath data association tracker for over-the-horizon radar," *IEEE Transactions on Aerospace and Electronic Systems*, vol. 34, no. 4, pp. 1165–1183, 1998.

[8] B. S. Karunaratne, M. Morelande, B. Moran, and S. Howard, "Performance bounds for tracking in a multipath environment," in *IEEE International Conference on Acoustics, Speech and Signal Processing (ICASSP)*, 2011, pp. 3652–3655.

[9] B. S. Karunaratne, Mark Morelande, and Bill Moran, "Target tracking in a multipath environment," in *IET International Conference on Radar Systems (Radar)*, Glasgow, UK, 2012, pp. 1–6.

[10] B. S. Karunaratne, M R Morelande, and B. Moran, "MCMC particle filter for tracking in a partially known multipath environment," in *IEEE International Conference on Acoustics, Speech and Signal Processing (ICASSP)*, Vancouver, BC, 2013, pp. 6332–6336.

[11] H.F. Durrant-Whyte and T Bailey, "Simultaneous Localization and Mapping: Part I," *Robotics & Automation Magazine*, pp. 99–108, June 2006.

[12] T Bailey and H.F. Durrant-Whyte, "Simultaneous localization and mapping (SLAM): Part II," *IEEE Robotics & Automation Magazine*, pp. 108–117, Sept. 2006.

[13] L Li and J.L. Krolik, "Target tracking in uncertain multipath environments using Viterbi Data Association," *IEEE International Conference on Information Fusion*, pp. 1–7, 2011.

[14] Y. Bar-Shalom, F Daum, and J Huang, "The probabilistic data association filter," *IEEE Control Systems Magazine*, pp. 82–100, Dec. 2009.

[15] L Svensson, D Svensson, and P Willett, "Set JPDA algorithm for tracking unordered sets of targets," in *IEEE International Conference on Information Fusion*, 2009, pp. 1187–1194.

[16] M. S. Arulampalam, S Maskell, N. Gordon, and T. Clapp, "A tutorial on particle filters for online nonlinear/non-Gaussian Bayesian tracking," *IEEE Transactions on Signal Processing*, vol. 50, no. 2, pp. 174–188, 2002.

[17] N Oudjane and C Musso, "Progressive correction for regularized particle filters," in *IEEE International Conference on Information Fusion*, 2000.

[18] S S Blackman, "Multiple hypothesis tracking for multiple target tracking," *Aerospace and Electronic Systems Magazine, IEEE*, vol. 19, no. 1, pp. 5–18, 2004.